

Highly Solar Radiation Reflective  $\text{Cr}_2\text{O}_3\text{-3TiO}_2$  Orange Nanopigment Prepared by a Polymer-Pyrolysis MethodYuan-Qing Li,<sup>\*,†,‡</sup> Shi-Gang Mei,<sup>†</sup> Young-Ji Byon,<sup>§</sup> Jian-Lei Wang,<sup>†</sup> and Guang-Lei Zhang<sup>†</sup><sup>†</sup>School of Materials Science and Engineering, Shijiazhuang Tiedao University, Shijiazhuang 050043, China<sup>‡</sup>Aerospace Engineering and <sup>§</sup>Civil Engineering, Khalifa University of Science Technology and Research, Abu Dhabi 127788, UAE

**ABSTRACT:** The present study reports the preparation and characterization of an orange nanopigment with high solar radiation reflective properties. Complex  $\text{Cr}_2\text{O}_3\text{-3TiO}_2$  nanoparticles were prepared by the pyrolysis of Cr–Ti precursors at high temperature, and the effects of the calcination temperature on the structure of  $\text{Cr}_2\text{O}_3\text{-3TiO}_2$  nanopigment were investigated by thermal analysis, X-ray diffraction, and transmission electron microscopy. The results reveal that the  $\text{Cr}_2\text{O}_3\text{-3TiO}_2$  pigments having rutile structure can be prepared by the calcination of the precursor at above 600 °C. All  $\text{Cr}_2\text{O}_3\text{-3TiO}_2$  pigments are granular in nature and present a homogeneous particle size of around 20 nm. The ultraviolet–visible near infrared (UV–vis–NIR) reflection spectra show that the  $\text{Cr}_2\text{O}_3\text{-3TiO}_2$  nanopigments have a reflection peak at around 600 nm, which reflects the orange color of these pigments. The average reflectance of  $\text{Cr}_2\text{O}_3\text{-3TiO}_2$  in the NIR range is around 53%, respectively, which is much higher than that of the visible light range. The prepared orange  $\text{Cr}_2\text{O}_3\text{-3TiO}_2$  nanopigments have a great potential in applications such as cool materials used for buildings with energy saving performance.

**KEYWORDS:** Orange pigment, Reflective, Solar, Polymer-pyrolysis



## INTRODUCTION

The incidence of the urban heat island (UHI), a phenomenon caused mainly by the removal of natural vegetation and its replacement with buildings and paved surfaces, is increasing in large metropolitan centers and produces temperatures exceeding 10 °C above those in surrounding areas.<sup>1</sup> The UHI has the effect of increasing energy consumption, particularly by the air conditioners that are widely used in large buildings in hot seasons. The use of highly reflective “cool” materials helps in maintaining lower exterior surface temperatures of buildings and consequently contributes toward increasing indoor thermal comfort levels, resulting in reduction of energy need for cooling.<sup>1–3</sup>

The reflective cool materials, usually bright white, can remain approximately up to 30 °C cooler than traditional materials during peak summer conditions. Such as  $\text{TiO}_2$ , a white pigment with a high solar reflectance of about 87%, is currently regarded as the best pigment for cool materials.<sup>4</sup> However, cool colored materials are often preferred for the cases where the use of light colors creates glare problems or when the aesthetics of darker colors is preferred.<sup>3,5,6</sup> Complex inorganic color pigments, which reflect near-infrared (NIR) radiation irrespective of the selective visible light reflection/adsorption and thus may be in any color, have well-known applications in masking products, interior car paint, materials for spectator areas of stadiums, and parking areas to fire-resistant paints,<sup>4,7,8</sup> and moreover, they are also used specifically in cool materials for exterior surface of buildings. Chromium oxide ( $\text{Cr}_2\text{O}_3$ ), green pigment with a medium high NIR reflectance in the range of 50–57%, is a good candidate to make nonwhite cool materials.<sup>9,10</sup> On the

basis of  $\text{Cr}_2\text{O}_3$ , different complex color pigment systems with excellent reflectance have been developed, such as green, gray, and black.<sup>9–13</sup> However, very few studies report orange pigments based on  $\text{Cr}_2\text{O}_3$ .

In recent years, the polymer pyrolysis method has been developed by our group for preparation of semiconductor and pigment nanoparticles.<sup>14–16</sup> When compared with solid state reaction methods, the conventional method of synthesis of ceramic pigments, the polymer pyrolysis method has some advantages: (a) easy to get nanoscale particles, which possess better solar reflectance than traditional microscale pigments, (b) easy to operate, no need of milling or sieving to adjust particle size, and (c) easy to scale-up in batch form.<sup>7,17,18</sup> In this paper, the preparation of  $\text{Cr}_2\text{O}_3\text{-3TiO}_2$  nanopigments by pyrolyzing Cr–Ti precursor is reported. The  $\text{Cr}_2\text{O}_3\text{-3TiO}_2$  pigments prepared show brilliant orange color with particle size of around 20 nm and high NIR reflectance above 50%. The orange  $\text{Cr}_2\text{O}_3\text{-3TiO}_2$  nanopigment prepared has great potentials in applications for energy saving buildings as cool materials.

## EXPERIMENTAL SECTION

**Preparation of  $\text{Cr}_2\text{O}_3\text{-3TiO}_2$  Nanopigments.** The chemical reagents tetra-*n*-butyl titanate ( $\text{Ti}(\text{C}_4\text{H}_9\text{O})_4$ ), chromium(III) acetate ( $\text{Cr}(\text{CH}_3\text{COO})_3$  50% solution, ammonium persulfate ( $(\text{NH}_4)_2\text{S}_2\text{O}_8$ ), and acrylic acid ( $\text{CH}_3\text{COOH}$ ) are analytical grade and used without

Received: September 20, 2013

Revised: October 20, 2013

Published: October 28, 2013

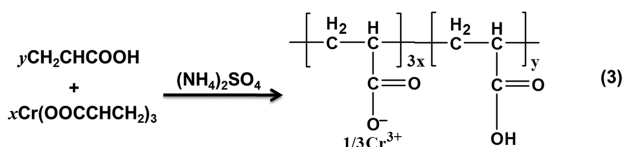
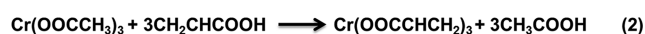
further purification processes. In a typical experiment,  $\text{Cr}(\text{CH}_3\text{COO})_3$  (0.002 mol) and  $\text{Ti}(\text{C}_4\text{H}_9\text{O})_4$  (0.003 mol) were added into 20 g of  $\text{CH}_3\text{COOH}$  aqueous solution ( $\text{CH}_3\text{COOH}:\text{H}_2\text{O} = 70:30$  wt %) under magnetic stirring. Afterward, a small amount (1 g) of 5 wt %  $(\text{NH}_4)_2\text{S}_2\text{O}_8$  aqueous solution as initiator was added to the mixed  $\text{CH}_3\text{COOH}$  solution to promote the polymerization. Under heating at  $90^\circ\text{C}$ , the mixed solution was stirred for 20 min to form the well-distributed polyacrylate precursor. The obtained precursor was dried at  $200^\circ\text{C}$  for 2 h and, then, calcined at  $600$  and  $800^\circ\text{C}$  for 2 h, respectively. Finally, the obtained orange  $\text{Cr}_2\text{O}_3\text{-}3\text{TiO}_2$  nanopigments were denoted as  $\text{Cr}_2\text{O}_3\text{-}3\text{TiO}_2\text{-}600$  and  $\text{Cr}_2\text{O}_3\text{-}3\text{TiO}_2\text{-}800$ , respectively.

**Characterization.** Thermogravimetry and differential scanning calorimetry (TG-DSC) analysis was performed using a NETZSCH STA 409PC instrument under air in the temperature range of  $30\text{--}800^\circ\text{C}$  at a heating rate of  $10^\circ\text{C}/\text{min}$ . X-ray diffraction (XRD) patterns were recorded on a Bruker D8 ADVANCE X-ray diffractometer at a voltage of 40 kV with  $\text{Cu K}\alpha$  radiation ( $\lambda = 1.5406 \text{ \AA}$ ) in the  $2\theta$  ranging from  $15^\circ$  to  $75^\circ$ .

Transmission electron microscopy (TEM) of  $\text{Cr}_2\text{O}_3\text{-}3\text{TiO}_2$  samples was performed on a transmission electron microscope (Model JEM-2100, Hitachi) and the particle sizes from TEM were estimated with a software (Photoshop 7.0). The optical properties of the  $\text{Cr}_2\text{O}_3\text{-}3\text{TiO}_2$  nanoparticles were studied using an ultraviolet-visible-near-infrared (UV-vis-NIR) spectrophotometer (Varian, Cary 5000) with integrating sphere. The reflection spectra were scanned in the range of  $250\text{--}2500$  nm with a 1-nm interval.

## RESULTS AND DISCUSSION

$\text{Cr}_2\text{O}_3\text{-}3\text{TiO}_2$  nanopigments were prepared by a polymer-pyrolysis method. The polymeric precursors were made by in situ polymerization of the mixed aqueous solution of acrylic acid in the presence of metal salt with  $(\text{NH}_4)_2\text{S}_2\text{O}_8$  as the initiator. This affords a composition which has the predetermined ratio of Cr to Ti (2:3) to be compatible with the final product ( $\text{Cr}_2\text{O}_3\text{-}3\text{TiO}_2$ ) according to the following reactive formula.



In the above formula,  $x$  and  $y$  represent the molar ratio of  $\text{Cr}(\text{CH}_3\text{COO})_3$  and  $\text{CH}_2\text{CHCOOH}$ , respectively. When the value of  $x$  is close to  $y$ , the polymerization reaction is difficult to initiate, and lead to ill-defined products. Thus, it is necessary to choose starting materials with  $x \ll y$ .<sup>15,16,19</sup> With the existence of a large amount of  $\text{H}_2\text{O}$ ,  $\text{Ti}(\text{C}_4\text{H}_9\text{O})_4$  mainly hydrolyze with the water in situ and lead to an immediate nucleation of  $\text{Ti}(\text{OH})_4$ , which is distributed randomly within the polymer precursor, as shown in Figure 1. The Cr (III) ions are bound by the ionic bonds between the metallic ions and carboxylate ions in a polymeric chain or between the polymeric chains. This uniform distribution of Cr (III) ions and  $\text{Ti}(\text{OH})_4$  in the precursor is key to the formation of  $\text{Cr}_2\text{O}_3\text{-}3\text{TiO}_2$  complex pigment in the following pyrolysis process.

As shown in Figure 2, the compositional and structural changes of copolymeric precursors associated with a thermal pyrolysis process are characterized using TG-DSC. The TG curve reveals that the weight loss proceeds in three different

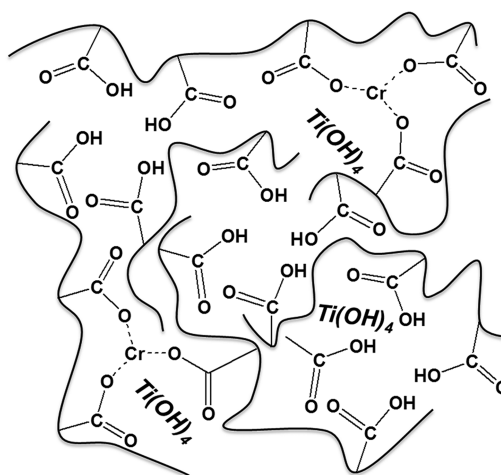


Figure 1. Schematic representation of polymeric precursor.

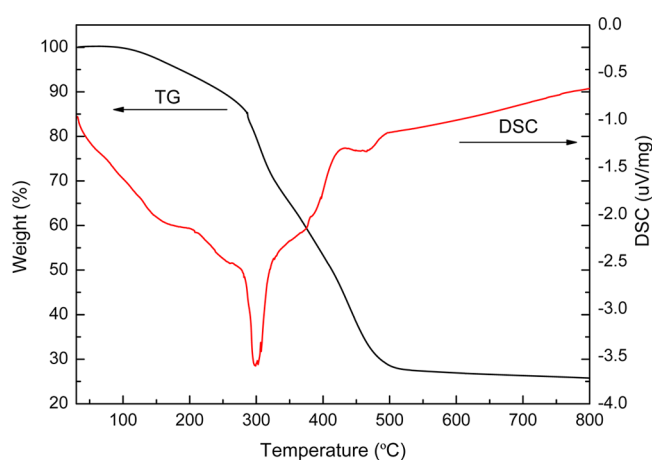
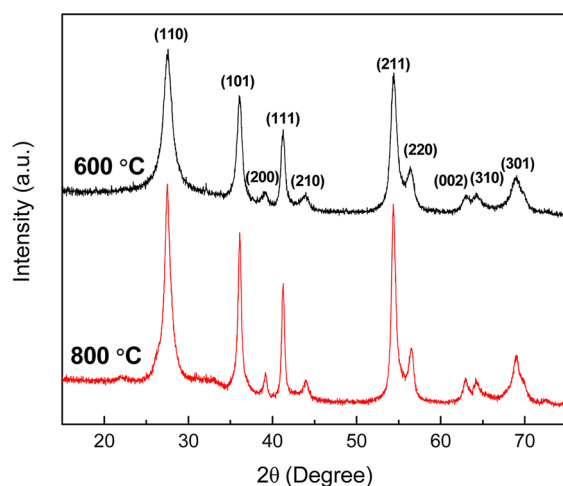


Figure 2. TG-DSC curves of  $\text{Cr}_2\text{O}_3\text{-}3\text{TiO}_2$  precursor.

stages with increasing temperature and that the total weight loss is about 74%. From the room temperature to around  $300^\circ\text{C}$ , the mass of polymer precursor decreases gradually with about 15% loss, which is associated with the removal of the residual water, acetate and unpolymerized acrylic acid molecular in the precursor. Most significant weight loss occurs in the temperature range of  $300$  to  $500^\circ\text{C}$ , and more than 55% of the mass is lost at this stage, which is associated the pyrolysis of precursor into  $\text{Cr}_2\text{O}_3\text{-}3\text{TiO}_2$  complex pigment. It is also observed that a high exothermic peak occurs at around  $300^\circ\text{C}$ , indicating the transformation of the precursor to  $\text{Cr}_2\text{O}_3\text{-}3\text{TiO}_2$ . It should be noted that the weight is almost unchanged above  $600^\circ\text{C}$ , indicating the formation of  $\text{Cr}_2\text{O}_3\text{-}3\text{TiO}_2$  nanoparticles. Hence,  $600$  and  $800^\circ\text{C}$  was optimized as the calcination temperature in preparation of  $\text{Cr}_2\text{O}_3\text{-}3\text{TiO}_2$  pigments, respectively.

Figure 3 displays XRD patterns of  $\text{Cr}_2\text{O}_3\text{-}3\text{TiO}_2$  pigments calcined in air at different temperature. It is clear that the main diffraction peak positions of pigments calcined at  $600$  and  $800^\circ\text{C}$  both present a pure rutile phase. In the traditional solid-state method, obtaining a pure rutile phase is difficult in this temperature range. Generally, anatase-to-rutile transformation occurred at  $900^\circ\text{C}$  for the traditional method, and pure rutile was detected at  $1000^\circ\text{C}$ .<sup>20</sup> Although with a high Cr content (40 mol %), no  $\text{Cr}_2\text{O}_3$  related phases are seen in any of the samples, indicating that Cr ions diffused completely into the



**Figure 3.** XRD patterns of  $\text{Cr}_2\text{O}_3$ - $3\text{TiO}_2$  nanoparticles with different calcinations temperature.

rutile lattice. Previous results also reveal that phase separation between  $\text{TiO}_2$  and  $\text{Cr}_2\text{O}_3$  can be observed only when Cr content is higher than 50 mol %.<sup>21</sup> In addition, all diffraction peaks are broadened, indicating the size of obtained samples in nanoscale. The peaks became sharper and more intense as the calcination temperature increased, indicating improved crystallization and increased crystallite size. For  $\text{Cr}_2\text{O}_3$ - $3\text{TiO}_2$ -600 and  $\text{Cr}_2\text{O}_3$ - $3\text{TiO}_2$ -800, the average particle sizes calculated from the Scherrer equation are 14.1 and 20.3 nm, respectively.<sup>22</sup>

The morphology and particle sizes of  $\text{Cr}_2\text{O}_3$ - $3\text{TiO}_2$  pigments prepared can be observed by TEM. As shown in Figure 4, all  $\text{Cr}_2\text{O}_3$ - $3\text{TiO}_2$  samples are granular in nature and

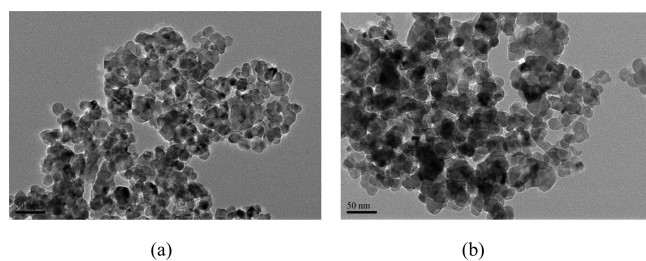


**Figure 4.** TEM images of  $\text{Cr}_2\text{O}_3$ - $3\text{TiO}_2$  nanoparticles with different calcinations temperature: (a) 600 and (b) 800 °C.

present a homogeneous nanoscale particle size. Excellent dispersion is observed in all samples with a narrow grain sizes with the distribution in the range of 10–100 nm. In addition, the grain size slightly increases with an increase of calcination temperatures. For  $\text{Cr}_2\text{O}_3$ - $3\text{TiO}_2$ -600 and  $\text{Cr}_2\text{O}_3$ - $3\text{TiO}_2$ -800, the average particle sizes are 16.7 and 24.7 nm, respectively. These results are in a good agreement with the crystallite sizes calculated by the XRD technique, the particle size of  $\text{Cr}_2\text{O}_3$ - $3\text{TiO}_2$  increases with increasing calcination temperature. Thus, the particle sizes of  $\text{Cr}_2\text{O}_3$ - $3\text{TiO}_2$  nanoparticles are adjustable by controlling the calcination temperature. In the traditional solid-state reaction method, the calcined products must be milled and sieved to adjust the grain size of the ceramic pigments, and only microscale pigment particles can be obtained.<sup>20</sup> In the present work, nanoscale pigment can be prepared directly by the high temperature pyrolysis polymer precursor, without requiring milling or sieving.

For the  $\text{Cr}_2\text{O}_3$ - $3\text{TiO}_2$  complex pigment, Cr is inserted into the  $\text{TiO}_2$  (rutile) lattice, the electronic transitions of Cr ions result in substantial absorption in the visible region. The UV-vis-NIR reflection spectra of  $\text{Cr}_2\text{O}_3$ - $3\text{TiO}_2$  prepared are shown in Figure 5, and both samples show three distinct absorption

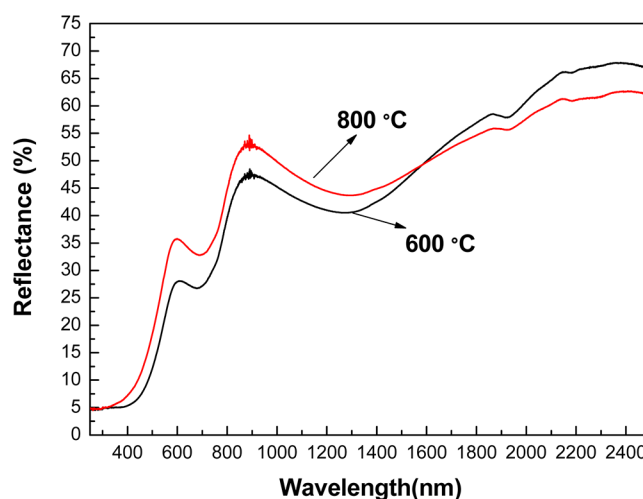


**Figure 5.** UV-vis-NIR spectra of  $\text{Cr}_2\text{O}_3$ - $3\text{TiO}_2$  pigments.

bands between 250 and 1600 nm. The absorption band less than 600 nm is attributed to the charge transfer band of  $\text{Cr(III)} \rightarrow \text{Ti(IV)}$  and parity-forbidden transitions of  $\text{Cr(III)}$  in octahedral coordination. The presence of the  $\text{Cr}^{3+}$  ions caused significant shifts of absorption bands into the visible region compared to the absorption threshold of pure  $\text{TiO}_2$  near 400 nm.<sup>23</sup> The two weak absorption peaks located around 680 and 1300 nm are due to Cr (III) spin forbidden transitions.<sup>20</sup> In addition, it can be observed that the  $\text{Cr}_2\text{O}_3$ - $3\text{TiO}_2$  pigments have a reflection peak in  $\sim 600$  nm, which reflects the color of these pigments. As shown in Figure 6, the  $\text{Cr}_2\text{O}_3$ - $3\text{TiO}_2$



**Figure 6.** Images of  $\text{TiO}_2$  and  $\text{Cr}_2\text{O}_3$ - $3\text{TiO}_2$ -600 nanopigments.

pigments prepared show a deep and brilliant orange color when compared with the white  $\text{TiO}_2$ , which has great potential application when the aesthetics of darker colors is preferred.

The sunlight, although it is more intense in the visible range, also emits a substantial amount of energy in the invisible UV and NIR range. In fact, about half of all solar power arrives as invisible NIR radiation, which results in the heat built-up on the surface of buildings.<sup>5,24</sup> As shown in Figure 5, a reflection peak in  $\sim 890$  nm and a broad reflection band above 1400 nm are seen in the NIR range (800–2500 nm), it is obvious that the reflectance of  $\text{Cr}_2\text{O}_3$ - $3\text{TiO}_2$  in the NIR range is much higher than that of the visible light range (400–800 nm). The average reflectance of  $\text{Cr}_2\text{O}_3$ - $3\text{TiO}_2$  in NIR range and visible light range is around 53% and 25%, respectively. Furthermore, in the

visible light range, the reflectance of  $\text{Cr}_2\text{O}_3\text{-3TiO}_2\text{-800 } ^\circ\text{C}$  is higher than  $\text{Cr}_2\text{O}_3\text{-3TiO}_2\text{-600 } ^\circ\text{C}$  due to the particle size effect. However, in the NIR range (above 1600 nm), the trend is reversed. The reflectance of  $\text{Cr}_2\text{O}_3\text{-3TiO}_2\text{-800}$  is higher than that of  $\text{Cr}_2\text{O}_3\text{-3TiO}_2\text{-600}$ . A similar phenomenon has been also reported in of  $\text{NiTiO}_3$  pigments.<sup>14</sup> Although the NIR reflectance of  $\text{Cr}_2\text{O}_3\text{-3TiO}_2$  is lower than white  $\text{TiO}_2$  (87%), it is comparable with green  $\text{Cr}_2\text{O}_3$  pigment (50–57%). The replacement of conventional orange pigments in commercial paint formulations with cool  $\text{Cr}_2\text{O}_3\text{-3TiO}_2$  pigments that absorb less NIR radiations allows the development of products with similar in color but high solar reflectance. Consequently, cool coatings absorb less solar energy, which keeps the building surface at a lower temperature and decreases energy transfer by radiation.

## CONCLUSIONS

In this paper, orange nanopigments  $\text{Cr}_2\text{O}_3\text{-3TiO}_2$  having a high NIR solar reflectance for building surface materials have been developed. Pigment nanoparticles were prepared by pyrolysis of Cr–Ti polymeric precursors via in situ polymerization. Thermal analysis and XRD measurements reveal that the  $\text{Cr}_2\text{O}_3\text{-3TiO}_2$  pigments with rutile structure can be prepared by calcination of the precursor at above 600 °C. All  $\text{Cr}_2\text{O}_3\text{-3TiO}_2$  samples are granular in nature and present a homogeneous particle size of around 20 nm. The UV–vis–NIR reflection spectra show that the  $\text{Cr}_2\text{O}_3\text{-3TiO}_2$  pigments have a reflection peak in ~600 nm, which reflects the orange color of these pigments. The average reflectance of  $\text{Cr}_2\text{O}_3\text{-3TiO}_2$  in the NIR range is around 53%, which is much higher than that of the visible light range. The prepared orange  $\text{Cr}_2\text{O}_3\text{-3TiO}_2$  nanopigments are promising materials for preparing building coatings with energy saving performance.

## AUTHOR INFORMATION

### Corresponding Author

\*Tel.: +971-(0)2-5018418. E-mail address: yqli@mail.ipc.ac.cn.

### Notes

The authors declare no competing financial interest.

## ACKNOWLEDGMENTS

The financial support of this work by the Natural Science Foundation of Hebei Province, China (Grant No.: E2012210014) is gratefully acknowledged.

## REFERENCES

- (1) Uemoto, K. L.; Sato, N. M. N.; John, V. M. Estimating thermal performance of cool colored paints. *Energy Build.* **2010**, *42* (1), 17–22.
- (2) Synnefa, A.; et al. Experimental testing of cool colored thin layer asphalt and estimation of its potential to improve the urban microclimate. *Build. Environ.* **2011**, *46* (1), 38–44.
- (3) Levinson, R.; et al. Methods of creating solar-reflective nonwhite surfaces and their application to residential roofing materials. *Sol. Energy Mater. Sol. Cells* **2007**, *91* (4), 304–314.
- (4) Levinson, R.; Berdahl, P.; Akbari, H. Solar spectral optical properties of pigments - Part II: survey of common colorants. *Sol. Energy Mater. Sol. Cells* **2005**, *89* (4), 351–389.
- (5) Synnefa, A.; Santamouris, M.; Apostolakis, K. On the development, optical properties and thermal performance of cool colored coatings for the urban environment. *Solar Energy* **2007**, *81* (4), 488–497.
- (6) Levinson, R.; Akbari, H.; Reilly, J. C. Cooler tile-roofed buildings with near-infrared-reflective non-white coatings. *Build. Environ.* **2007**, *42* (7), 2591–2605.
- (7) Jeevanandam, P.; et al. Near infrared reflectance properties of metal oxide nanoparticles. *J. Phys. Chem. C* **2007**, *111* (5), 1912–1918.
- (8) Vishnu, V. S.; Reddy, M. L. Near-infrared reflecting inorganic pigments based on molybdenum and praseodymium doped yttrium cerate: Synthesis, characterization and optical properties. *Sol. Energy Mater. Sol. Cells* **2011**, *95* (9), 2685–2692.
- (9) Zhang, J.; et al. Near Infrared Reflectance of the Doped  $\text{Cr}_2\text{O}_3$  Pigment. *J. Inorg. Mater.* **2010**, *25* (12), 1303–1306.
- (10) Thongkanluang, T.; Kittiauchawal, T.; Limsuwan, P. Preparation and characterization of  $\text{Cr}_2\text{O}_3\text{-TiO}_2\text{-Al}_2\text{O}_3\text{-V}_2\text{O}_5$  green pigment. *Ceram. Int.* **2011**, *37* (2), 543–548.
- (11) Escardino, A.; et al. Kinetic study of black  $\text{Fe}_2\text{O}_3\text{-Cr}_2\text{O}_3$  pigment synthesis: I, influence of synthesis time and temperature. *J. Am. Ceram. Soc.* **2003**, *86* (6), 945–950.
- (12) Pishch, I. V.; Popovskaya, N. F.; Radion, E. V. Synthesis of pigments based on the  $\text{CuO-Cr}_2\text{O}_3\text{-Al}_2\text{O}_3$  system using the precipitation method. *Glass Ceram.* **1999**, *56* (9–10), 320–322.
- (13) De la Torre, A. G.; et al. Ceramic Pigments and the European REACH Legislation: Black  $\text{Fe}_2\text{O}_3\text{-Cr}_2\text{O}_3$ , a Case Study. *Int. J. Appl. Ceram. Technol.* **2011**, *8* (4), 905–910.
- (14) Wang, J. L.; et al. Synthesis and characterization of  $\text{NiTiO}_3$  yellow nano pigment with high solar radiation reflection efficiency. *Powder Technol.* **2013**, *235*, 303–306.
- (15) Li, Y. Q.; et al. Preparation and electrical properties of Ga-doped  $\text{ZnO}$  nanoparticles by a polymer pyrolysis method. *Mater. Lett.* **2010**, *64* (15), 1735–1737.
- (16) Li, Y. Q.; et al. Facile synthesis of antimony-doped tin oxide nanoparticles by a polymer-pyrolysis method. *Mater. Res. Bull.* **2010**, *45* (6), 677–681.
- (17) Gargori, C.; et al. In situ synthesis of orange rutile ceramic pigments by non-conventional methods. *Ceram. Int.* **2010**, *36* (1), 23–31.
- (18) Lopes, K. P.; et al.  $\text{NiTiO}_3$  powders obtained by polymeric precursor method: Synthesis and characterization. *J. Alloys Compd.* **2009**, *468* (1–2), 327–332.
- (19) Liu, X. M.; Yang, G.; Fu, S. Y. Mass synthesis of nanocrystalline spinel ferrites by a polymer-pyrolysis route. *Mater. Sci. Eng. C–Biomimetic Supramol. Syst.* **2007**, *27* (4), 750–755.
- (20) Zou, J. Low temperature preparation of Cr-doped rutile pigments with good colour properties. *Dyes Pigm.* **2013**, *97* (1), 71–76.
- (21) Jung, Y. S.; et al. Enhancement of photocatalytic properties of  $\text{Cr}_2\text{O}_3\text{-TiO}_2$  mixed oxides prepared by sol-gel method. *Curr. Appl. Phys.* **2011**, *11* (3), 358–361.
- (22) Li, Y. Q.; Fu, S. Y.; Mai, Y. W. Preparation and characterization of transparent  $\text{ZnO/epoxy}$  nanocomposites with high-UV shielding efficiency. *Polymer* **2006**, *47* (6), 2127–2132.
- (23) Jaimy, K. B.; et al. An aqueous sol-gel synthesis of chromium(III) doped mesoporous titanium dioxide for visible light photocatalysis. *Mater. Res. Bull.* **2011**, *46* (6), 914–921.
- (24) Sreeram, K. J.; et al. Colored cool colorants based on rare earth metal ions. *Sol. Energy Mater. Sol. Cells* **2008**, *92* (11), 1462–1467.